Extraction of surface image features for wear detection on ball screw drive spindles

Tobias Schlagenhauf, Max Heinzler, and Jürgen Fleischer

Karlsruhe Institute of Technology (KIT),
wbk Institute of Production Science,
Kaiserstraße 12, 76131 Karlsruhe

Abstract Failures of production machines are often caused by wear and the resulting failure of components. Therefore, condition-based monitoring of machines and their components is becoming an increasingly important factor in industry. Due to the simple conversion of the motion of electric rotary drives into precision feed motion, the ball screw is an inherent element of many production machines. Thus, a failure of the ball screw often leads to costly production stops. This paper shows the determination and extraction of wear-describing image features, allowing an image-based condition monitoring of ball screws using hyperparameter-optimized machine learning classifiers. The features to train the algorithms are derived and extracted based on the deep domain knowledge of ball screw drive failures in combination with further developed state of the art feature extraction algorithms.

Keywords Ball screw drive, image features, artificial intelligence, machine learning, pattern recognition

1 Introduction

The changes in the economic and technological environment force companies to constantly review their positioning in relation to their competitors and to search for innovations and competitive advantages. A decisive competitive advantage is an effective and efficient production. To avoid downtimes, the machines must be in perfect

condition [1]. A common goal in industry is to extend the lifecycle of production systems by early identification of defects and damages to machine parts. Such approaches are called Preventive and Predictive Maintenance. In the past, repairs and maintenance have been executed after machine breakdowns or a fixed period. Today, companies try to schedule repair and maintenance activities depending on the estimation of a machine's condition [2]. Knowing the right time to replace a machine's component is a desirable situation from a technical and economic perspective. If the components are changed too late, there will be a risk of damaging other machine elements or manufacturing faulty products, which in both cases will result in financial disadvantages. If the component is replaced too early, a certain part of its lifecycle will remain unused and unnecessarily premature financial expenses are incurred. A majority of machines used in the manufacturing process includes rotating components. Ball screws are the most frequently used design elements in today's machine tools for converting the motion of rotary electric drives into precision feed motions. Therefore, the functionality of a machine depends on the ball screw and a failure can lead to a costly production stop [3]. Typical reasons for such defects are abrasion by foreign particles, adhesion due to cold welding and surface disruption. Surface disruption occurs during application and results in pittings. Pittings are a common reason for ball screw failure, so the aim of this study is to detect this wear automatically.

In literature, the condition of a ball screw is often analyzed through vibration. As described in [4] and [5], most mechanical systems generate vibration signals that provide information about the state of a system. The more relevant approaches for this work are the image-based methods of defect analysis. Approaches from other metallic surfaces than spindles are also considered to investigate further possible solutions. A frequently applied method is the use of deep learning algorithms. In most cases, these approaches are based on a convolutional neural network (CNN). As described in [6] and [7], this technique has already been successfully applied to ball screws to detect pitting using a CNN. The classification accuracy of [6] is just over 90% and that of [7] is even higher at 99%. [8] adopt the deep learning approach to analyze image data for the identification of rail surface defects. The algorithm also classifies

among various defect conditions (normal, weld, light squat, moderate squat, heavy squat and joint). The results of the approach prove the efficiency with a classification accuracy of almost 92%. Another CNN-based approach is published by [9]. This method has also been developed to monitor defects in the rail system.

Deep learning is an effective approach with the disadvantage of lacking traceability of the decision making process. The extraction of image features using domain knowledge and subsequent classification increases the transparency of decision making.

2 Ball screw drive image features

The first subject is the preparation of the image data set. It is important to create a comprehensive data set in order to be able to record as much optical characteristics as possible. Since pittings occur in the thread raceway, it is the region of interest (ROI). The thread ridges have a strong optical characteristic and are therefore not included in the data set. As a result, only the thread raceways are extracted. Also, a suitable image size must be selected in order to be able to analyze as much ROI information as possible. This leads to an image resolution for the single images of 128x128 pixels and the data set size is 1000 images per class (pitting and no pitting).

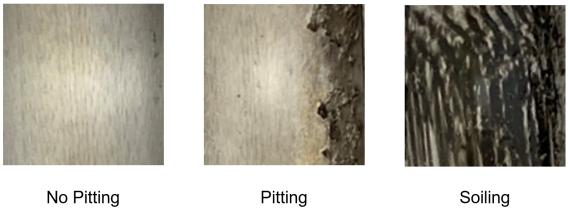

Figure 2.1: Sample images from the data set

A main task of the paper is to extract features from the wear patterns of the ball screw with image filter methods based on domain knowledge. The challenge is the automatic detection of wear on the spindle (Pittings) despite oil residues on the ball screw spindle. Since soiling has a strong optical characteristic, it must be also con-

sidered in detail and thus represents the third class in the analysis besides pitting and no pitting (see Table 1). For classification, only the classes pitting and no pitting are used. The elaborated characteristics are assigned to the image feature categories color, shape and texture. Pittings occur in the raceway, so only this area of the spindle is considered in the analysis. Figure 2.1 shows a sample images from the data set without pitting, an image with pitting and an image with soiling.

Since color features are invariant to scaling, translation and rotation, they have a major impact on image analysis. The spindle surface, soiling and pittings are exclusively brown and grey shades, which is why the share of red, green and blue (RGB) is almost equal. A surface of a spindle raceway without pitting and without soiling is characterized by having almost exclusively bright brown and grey shades. A significant difference can be detected in the images with pitting. Because of the dark pittings, the image is not composed exclusively of bright colors like the image without them. The soiling on the spindle is usually oil residues, therefore, it is typically black or grey. In the case of heavy soiling, oil residues can cover the entire raceway, so that the color composition consists mainly of very dark shades. Due to the nearly identical color of pitting and soiling, an almost similar histogram can be determined for an image without pitting, but soiling. For this reason, texture and shape features are determined in addition to the color features.

A spindle without pitting usually has a uniform raceway structure. The surface has hardly any or no contrast differences. The balls of the ball screw result in a slight vertical structure in the running direction. To a great extent, this structure is also evident in the image with pittings. Pittings have an uneven structure with a strong contrast difference to the rest of the raceway. The texture in the area of the pitting appears partially plateau-like, interspersed with dark spots. Pittings are not uniform but have varying degrees of protrusion into the rest of the material without pittings. Since soiling is random, there are often many local and global contrast differences and the surface can have a random and/or uniform texture. However, soiling often follows the vertical running direction of the screw drive as shown in the sample image (see Figure 2.1). Soiling is the major unknown factor in the texture analysis due to its random occurrence.

Considering the raceway of a spindle without pitting, no noticeable shapes can be identified. With pitting and soiling, it is not the shape itself that is decisive, as soiling can have similar contours to pittings, but the location of the shape is an indication of the respective class. Pittings always occur in the flanks of the spindle raceways, while soiling usually spreads over the entire surface or occurs in the middle area of the raceway. Due to the knowledge of the occurrence of soiling and pittings, the shape features are ideally suited as spatial features.

Table 1: Differences No Pitting/Pitting/Soiling based on domain knowledge

No Pitting	Pitting	Soiling	Feature Category
Light brown, grey	Dark brown shades	Black, grey	Color
Few color shades	Many different color shades	Few color shades	Color
No colored line	Partly colored line next to pitting	No colored line	Color
Regular surface	Irregular surface	Uniformity of the surface depends on the degree of soiling	Texture
Few contrast differences	Many global/local significant differences in contrast	Significant differences in contrast; quantity depends on the degree of soiling	Texture
Even texture	Random texture	Texture runs in the direction of the thread balls	Texture
No plateau-like texture	Plateau-like/"Map"	No plateau-like texture	Texture
Hardly any edges	Many edges	(Mostly) many edges	Shape
-	Occurs on the flank	Occurs randomly; usually spread over the entire surface	Spatial

3 Feature extraction

Table 1 is fundamental for the following development of the extraction methods. The methods are intended to extract a variety of characteristics from this table.

3.1 Color Features

Each image contains 49152 color values (128x128 pixels × RGB values). The extraction approach for the color features focuses on simplifying and clustering the data. To cluster the image colors an own approach based on [10] is develpoed. The K-Means algorithm is applied and the pixels are assigned to a defined number of clusters. The color of a cluster is defined by its centroid. With this method, the color properties are displayed in a more compact form but to capture a wide color spectrum of an image, a high number of clusters must be defined. Therefore, the number of clusters is set to 20. To describe the relationship between color and distribution of the clusters the own approach "Clustered Color Share (CCS)" is applied. Since the RGB values for each cluster are almost identical due to the predominantly grey or brown colors of the data set images, the RGB mean value of the centroid is calculated. Afterwards, the averaged RGB value of the centroid is multiplied with the cluster's share. This way the color as well as the share can be represented in one feature. The progression of the twenty features and the feature values can be used to identify the composition of the color in an image. The mean value, median value, maximum value, minimum value and standard deviation of the RGB mean values are additionally included as features in the feature vector.

3.2 Texture Features

As a result of the high complexity of the texture, two approaches from literature are applied and examined. The first approach combines the grey-level co-occurrence matrix and the Haralick features [11] to compute a global representation of the texture. Initially, the four grey-level co-occurrence matrices are calculated and afterwards,

the Haralick features are determined. The feature vector is the average of the result vectors of the individual matrices. For this purpose, a matrix with the 13 Haralick features is created and the feature vector for the images is calculated.

The second approach uses the Local Binary Patterns (LBP) [12] to compute a local representation of texture. The first step is to create the LBP matrix for the image. For this purpose, a 3x3 pixels neighbourhood is chosen for each pixel. Following the calculation of the matrix, the first and last columns as well as rows are truncated because no calculation is possible for these pixels as they have no 3x3 neighbourhood. Afterwards, the frequency of the individual LBP patterns can be determined and saved as feature vector. As additional features, the statistical properties mean, median, minimum and maximum of the feature vector are appended.

3.3 Shape/Spatial Features

The extraction of the shape features is based on the SIFT algorithm published by [13]. The SIFT method enables the search for features that are invariant to rotation, translation, scaling, changes in light conditions and partially affine distortion [13]. However, the resulting derivation of the shape/spatial feature and the extraction of the feature vector is the own approach "KeyPoints Per Sub Region (KPPSR)". Since pittings occur on the flanks of a spindle, the shape features are ideally suited to describe the spatial variable of pittings. The position and number of KeyPoints extracted from the SIFT algorithm are used to describe this characteristics. The number and location of the KeyPoints can provide information about the structure and shape of the object (see Figure 3.1).

As exemplarly shown in Figure 3.1 the distribution of the KeyPoints over sub regions is an important characteristic to distinguish between pitting and no pitting images. The shape of the oil residues leads to a strong accumulation of KeyPoints over the entire image. To analyze the differences between the inner and the outer regions of the image, the image is divided into 4x4 sub regions and the SIFT algorithm is applied. After the segmentation of the image into sub regions, the feature vector can be determined. Thereby, the sub regions form a matrix. The regions are numbered (from 0 to 3) in x

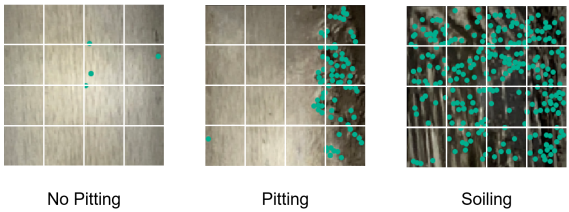

Figure 3.1: Scheme "KeyPoints per Sub Region"

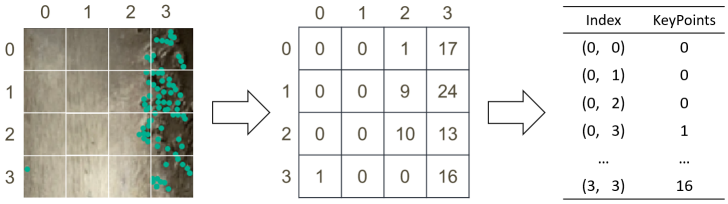

Figure 3.2: Example "KeyPoints per Sub Region"

and y direction resulting in each region having a unique index value (see Figure 3.2).

4 Results

Overall, 28 color features, 274 texture features (261 LBP, 13 Haralick) and 16 shape features are extracted. To verify the performance of the extracted features, three-layer neural networks are applied to the individual methods. Since the optimal number of neurons per layer, the optimal activation function and the optimal solver can be different for each feature, 100 randomly generated combinations are applied to the features. Due to their stochastic nature, neural networks behave slightly different for each training. Therefore, each hyperparameter combination is applied five times. This means that a total of 500 neural networks are applied to the individual methods. All further tests are executed with the same split data sets. In total, the 2000 extracted feature data sets are randomly divided into 1600 training data sets (791 No Pitting and 809 Pitting) and 400 test data

sets (209 No Pitting and 191 Pitting). Table 2 shows the average fitness of the 500 neural networks, the average fitness of the ten best neural networks and the fitness of the best model.

Table 2: Results Methods

Method	Average Fit	AvgTop10	Best Fit
KPPSR	0,848	0,906	0,915
CCS	0,836	0,893	0,908
Haralick	0,847	0,939	0,950
LBP	0,836	0,929	0,935

All methods alone achieve classification accuracies of over 90%. The best results are achieved with texture features, followed by spatial features and color features. In the next step neural networks are applied to the combination of all features. Furthermore, the own approaches are replaced by existing approaches to compare the performance. For the analysis of the color features, a color histogram is selected and for the analysis of the KeyPoints the total number of KeyPoints in the image is used as feauture. Table 3 shows the average fitness of the 500 neural networks, the average fitness of the ten best neural networks and the fitness of the best model. The best result is achieved with KPPSR without CSS (but with color histogram) at a fitness of 98.8%.

Table 3: Results

KPPSR	CCS	Average Fit	AvgTop10	Best Fit
no	no	0,904	0,978	0,983
yes	no	0,921	0,986	0,988
no	yes	0,897	0,972	0,978
yes	yes	0,914	0,980	0,983

The number of possible combinations of parameter options for classification models are potentially infinite. For such optimization problems, exact methods like exhaustive searches become inefficient and heuristic methods become more suitable. One of these heuristic approaches is the Genetic Algorithm (GA) [14]. Therefore, in the

next step a genetic algorithm is applied to find the optimal hyperparameters for a neural network, which is applied to the extracted features (CCS, LBP, Haralick, KPPSR). The analogy to natural evolution enables genetic algorithms to overcome many of the hurdles that traditional search and optimization algorithms encounter. Especially when problems with a large number of parameters and complex mathematical representations are involved [14] [15]. Using the GA to optimize the hyperparameters of the neural net, classification accuracies of 98.8% can be achieved, which corresponds to the best fitness in Table 3.

In the last attempt, the image features of a spindle area (see Figure 4.1) are extracted and classified using the best-fit neural network. The individual images are recorded using the Sliding Window method. The four frames of the upper row are assigned with the label 0 to the class ”No Pitting” and the frames of the lower row are assigned with the label 1 to the class ”Pitting”. All images are assigned to the correct class.

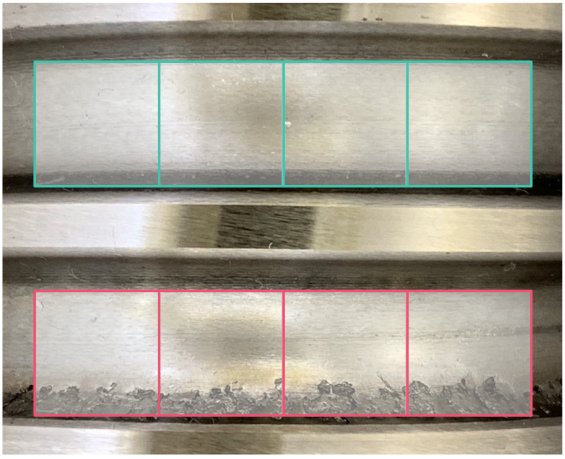

Figure 4.1: Sliding Window

5 Conclusion

Since the ball screw is used in most machines as electromechanical feed drive, the condition of the ball screw is critical for the operation of the machines. Early detection of wear on the spindle, and thus failures, helps to avoid production downtimes and reduce costs. The present approach shows that using a combination of the developed CSS and KPPSR methods together with methods from the literature, features can be extracted to properly classify 98.8% of the spindle surface images for pitting and no pitting. It can therefore be assumed that the selected extraction methods adequately describe the surface of a ball screw. This allows to react to failures at an early stage. Based on the data set, the texture features are the most important features due to the high classification accuracies (see Table 2), followed by the spatial features and color features. The results rely on selected methods and confirm the assumptions through domain knowledge. The hypothesis that texture features are the most important characteristics has to be validated by further experiments to make a general statement.

References

1. A. R. Mohanty, *Machinery Condition Monitoring - Principles and Practices*. Boca Raton, Fla: CRC Press, 2014.
2. D. G. Pascual, *Artificial Intelligence Tools - Decision Support Systems in Condition Monitoring and Diagnosis*. Hoboken: CRC Press, 2015.
3. A. Spohrer, "Steigerung der Ressourceneffizienz und Verfügbarkeit von Kugelgewindetrieben durch adaptive Schmierung," Ph.D. dissertation, Karlsruher Institut für Technologie (KIT), Karlsruhe, 2019.
4. W. G. Lee, J. W. Lee, M. S. Hong, S.-H. Nam, Y. Jeon, and M. G. Lee, "Failure diagnosis system for a ball-screw by using vibration signals," *Shock and Vibration*, 2015.
5. L. Zhang, H. Gao, J. Wen, S. Li, and Q. Liu, "A deep learning-based recognition method for degradation monitoring of ball screw with multi-sensor data fusion," *Microelectronics Reliability*, pp. 215–222, 2017.
6. T. Schlagenhauf, C.-P. Feuring, J. Hillenbrand, and J. Fleischer, "Camera based ball screw spindle defect classification system. System zur

kamerabasierten Defekterkennung auf Kugelgewindetriebspindeln," in *Production at the leading edge of technology. Proceedings of the 9th Congress of the German Academic Association for Production Technology (WGP), September 30th - October 2nd, Hamburg 2019*, J. P. Wulfsberg, W. Hintze, and B.-A. Behrens, Eds. Singapore: Springer Nature, 2019, pp. 503–512.

7. T. Schlagenhauf, P. Ruppelt, and J. Fleischer, "Detektion von frühzeitigen oberflächenzerrüttungen," *wt Werkstattstechnik online*, vol. 110, pp. 501–506, 2020. [Online]. Available: https://e-paper.vdi-fachmedien.de/webreader-v3/index.html#/2657/50
8. S. Faghih-Roohi, S. Hajizadeh, A. Nunez, R. Babuska, and B. d. Schutter, "Deep convolutional neural networks for detection of rail surface defects," *International Joint Conference 2016*, p. 2584–2589, 2016.
9. Y. Liu, X. Sun, and J. H. L. Pang, "A yolov3-based deep learning application research for condition monitoring of rail thermite welded joints," *Proceedings of the 2020 2nd 2020*, pp. 33–38, 2020.
10. K. Bhanot, "Color identification in images," *Towards Data Science*, 2018. [Online]. Available: https://towardsdatascience.com/color-identification-in-images-machine-learning-application-b26e770c4c71
11. R. M. Haralick, K. Shanmugam, and I. Dinstein, "Textural features for image classification," *IEEE Transactions on Systems, Man, and Cybernetics*, vol. SMC-3, no. 6, pp. 610–621, 1973.
12. T. Ojala, M. Pietikainen, and T. Maenpaa, "Multiresolution gray-scale and rotation invariant texture classification with local binary patterns," *IEEE Transactions on Pattern Analysis and Machine Intelligence*, vol. 24, no. 7, pp. 971–987, 2002.
13. D. G. Lowe, "Distinctive image features from scale-invariant keypoints," *International Journal of Computer Vision*, vol. 60, no. 2, pp. 91–110, 2004.
14. C. Rothwell, "Hyper-parameter optimisation using genetic algorithms: Classification task," 2018.
15. E. Wirsansky, *Hands-on genetic algorithms with Python: Applying genetic algorithms to solve real-world deep learning and artificial intelligence problems*. Birmingham, UK: Packt Publishing Ltd, 2020.